

A Novel Approach in Realistic Wind Data Generation for The Safe Operation of Small Unmanned Aerial Systems in Urban Environment

Rohit K. S. S. Vuppala* and Kursat Kara[†] School of Mechanical and Aerospace Engineering, Oklahoma State University, Stillwater, Oklahoma, 74075

In this study we present a preliminary work for a method to efficiently generate realistic wind data for urban environments using existing Large Eddy Simulation (LES) data for safe operation of small unmanned aerial vehicles. A single building setup in neutral atmospheric conditions is considered as a test case for demonstration of the method. The method relies on using Large Eddy Simulation data from a computational fluid dynamics simulation and a non-intrusive Reduced Order Modeling approach (ROM) coupled with Recurrent Neural Networks like Long Short Term Memory (LSTM). Proper Orthogonal Decomposition (POD) transform is used to extract modal coefficients from the high-resolution data snapshots and LSTM network is trained on a specific number of modal coefficients defined by their relative information content. Modal predictions for future time-steps are then obtained using this trained LSTM network, without the need of computationally expensive CFD simulations. The corresponding velocity fields for future time-steps are obtained by a inverse POD transform on these modal coefficients. Since no prior information about the underlying governing equations are utilized for the predictions, the method is a completely non-intrusive approach.

I. Nomenclature

 Θ, Θ_{ν} = potential temperature, virtual potential temperature

u, v, w =velocity components

 q_l, q_v = liquid water specific humidity, specific humidity

e = SGS turbulent kinetic energy

p = hydrostatic pressure

 C_p = specific heat constant at constant pressure

 R_v, R_d = gas constant for vapor and dry air L_v = Latent heat of vaporisation

II. Introduction

There has been an ever-increasing interest in recent years for Unmanned Air Vehicles (UAVs) due to their diverse applications and ease of access. As the complexity around these systems grew, so did the need to augment these vehicles with ground control stations (GCS), command and communication links, and other auxiliary subsystems. The term UAV is now outdated and replaced with Unmanned Air Systems (UAS) to better characterize these enhancements from using just the Unmanned Air Vehicles as a stand-alone system [1][2]. Recently, UAS applications have penetrated the civilian domain for various mission profiles like law enforcement[3], general reconnaissance, aerial structure inspection, disaster management[4], urban mapping[5] and in the near future delivery and catering services[6]. However there are significant, size and weight restrictions for many of these applications in the urban environment due to the urban ecosystem's dense nature. Small Unmanned Aircraft Systems have rapidly evolved to tackle these limitations, but they remain susceptible to external factors like wind, gusts, and turbulent wakes produced by urban structures. Atmospheric effects of urban environments have been the focus of researchers for many years yet, majority of them are restricted to meso-scale applications like climate predictions[7][8]. Recently they have been widely used for

^{*}Graduate Student, Mechanical and Aerospace Engineering, Oklahoma State University

[†]Assistant Professor, Mechanical and Aerospace Engineering, Oklahoma State University

urban applications like planning and mitigation of urban heat islands[9][10], pollution transport and dispersal[11] [12]. While recently researchers have investigated this influence on flight planning and trajectories [13][14] to develop various control strategies to minimize the effects, they face a significant challenge in testing algorithms with realistic wind data. Dryden and Von-Karman models have been widely used for modeling gusts but are limited to large domains with no structural elements or obstructions. While, Reynolds-Averaged Navier-Stokes(RANS) equations have been previously used to simulate the urban flow fields, they do not depict the unsteady nature of the flow field, especially in constricted spaces in urban environment. Large Eddy Simulations (LES), have enabled some progress in this regard since they provide a more accurate depiction of better wind data closely resembling realistic conditions[15] for testing UAV control algorithms [16]. But, Large Eddy Simulations are comparatively computationally expensive than RANS, and only limited research has been available for testing different flow scenarios[17] or for urban spaces[18]. Real-time prediction and flight correction strategies for UAS cannot be widely tested and adopted, given the inherent computational cost of LES.

Data-driven, Reduced Order Models (ROMs) are one efficient way to simulate fluid flow using available data and predict lower-order future flow fields. They have been used in many applications like process simulation and optimisation [19], flow control [20] and for fluid flows[21]. Researchers like Davoudi et al. have utilised this technique to develop a data-driven ROM from LES simulation data for realistic wind data reconstruction[22] at a fraction of computational cost. Using Proper Orthogonal Decomposition they could be relatively efficient, accurate, utilizing only a few important modes for reconstructing the flow field. With the advent of machine learning and artificial neural networks, they have been widely utilised for advancement in various flow modeling research[23] [24] [25] [26]. In this work we intend to use Machine Learning coupled with ROMs specifically, ROM-LSTMs[27] on the POD modes obtained from LES data for predicting wind fields. We choose a domain with a single building setup as a demonstration for its utility in urban wind prediction. This provides an effective method to generate more realistic wind data using previous high-fidelity LES data and without the need for expensive CFD simulations for all the time steps where data is needed for UAV testing and validation.

III. Methodology

In this section we discuss the methodology for our approach which uses Large Eddy Simulation data and non-intrusive ROM-LSTMs to predict the flow field in a given domain of interest.

A. LES simulation setup

Large Eddy Simulation data is obtained using Parallelized Large-Eddy Simulation Model (PALM)[28]. PALM is a turbulence-resolving, Large Eddy Simulation solver for atmospheric and oceanic boundary-layer flows. The model is based on solving non-hydrostatic, filtered, incompressible Navier-Stokes equations in Boussinesq-approximated form on a cartesian grid. Implicit separation of sub-grid scales and resolved scales is achieved by averaging the governing equations over discrete grid volumes as proposed by Schumann[29].

1. Governing Equations

The model solves for six prognostic quantities, the velocity components u, v, w, the potential temperature θ , specific humidity q_v and the SGS turbulent kinetic energy e. The potential temperature is defined as

$$\Theta = \frac{T}{\Pi} \tag{1}$$

from absolute temperature T and the Exner function,

$$\Pi = \left(\frac{p}{p_0}\right)^{\frac{R_d}{C_P}} \tag{2}$$

where, p is the hydrostatic pressure, p_0 is the reference pressure 1000 hPa, R_d is the gas constant for dry air and C_P is the specific heat of dry air at constant pressure. Furthermore a virtual potential temperature could be calculated using the relation,

$$\Theta_{\nu} = \Theta \left[1 + \left(\frac{R_{\nu}}{R_d} - 1 \right) q_{\nu} - q_l \right] \tag{3}$$

where R_{ν} is the gas constant for water vapor and q_{l} is the liquid water specific humidity calculated based on a chosen cloud micro-physics model. (Note: for the present study dry atmospheric boundary conditions with neutral stratification are considered eliminating the need for cloud multi-physics and also making the absolute temperature, potential temperature and virtual potential temperature the same value) The governing equations for the conservation of mass, momentum, energy and moisture filtered over a cartesian grid are expressed below in Einstein summation notation, where angle brackets denote horizontal domain average, over-bar indicates filtered quantities and double-prime indicates SGS variables.

$$\frac{\partial \overline{u_i}}{\partial t} = -\frac{\partial \overline{u_i} \overline{u_j}}{\partial x_j} - \varepsilon_{ijk} f_j \overline{u_k} + \varepsilon_{i3j} f_3 \overline{u}_{g,j} - \frac{1}{\rho_0} \frac{\partial \Pi^*}{\partial x_i} + g \frac{\overline{\Theta_v} - \langle \overline{\Theta_v} \rangle}{\langle \overline{\Theta_v} \rangle} \delta_{i3} - \frac{\partial \left(\overline{u_i'' u_j''} - \frac{2}{3} \overline{e} \delta_{ij}\right)}{\partial x_j}$$
(4)

$$\frac{\partial \overline{u_j}}{\partial x_i} = 0 \tag{5}$$

$$\frac{\partial \overline{\Theta}}{\partial t} = -\frac{\partial \overline{u_j} \overline{\Theta}}{\partial x_j} - \frac{\partial \left(\overline{u_j'' \Theta''} \right)}{\partial x_j} - \frac{L_v}{C_p \overline{\Pi}} \Psi_{q_v}$$
 (6)

$$\frac{\partial \overline{q_{\nu}}}{\partial t} = -\frac{\partial \overline{u_{j}q_{\nu}}}{\partial x_{j}} - \frac{\partial \overline{u_{j}'q_{\nu}''}}{\partial x_{j}} + \Psi_{q_{\nu}}$$
(7)

where.

 $u_i(i=1,2,3)$ represents the components of velocities, f_i is the Coriolis parameter, L_v is latent heat of vaporisation, g is the gravitational acceleration, $u_{g,k}$ are the geostrophic wind components, ρ_0 is the density of dry air, p^* is the perturbation pressure, $\Pi^* = p^* + 2/3\rho_0 e$ is the modified perturbation pressure, and SGS TKE is represented by e.

2. Turbulence closure

The closure includes a prognostic equation for the filtered SGS-TKE \bar{e} given below, the SGS terms are parametrized using 1.5 order closure following Deardorff[30], using a modified version of Wyngaard et al.[31] and Saiki et al.[32]. For further information regarding the parameterization of various terms in the equation, the reader is referred to [28].

$$\frac{\partial \overline{e}}{\partial t} = -\overline{u_j} \frac{\partial \overline{e}}{\partial x_j} - \overline{u_i^{"} u_j^{"}} \frac{\partial \overline{u_i}}{\partial x_j} + \frac{g}{\overline{\Theta_{v,0}}} \overline{u_3^{"} \Theta_{v}^{"}} - \frac{\partial \left[\overline{u_j^{"} \left(e + \frac{p^{"}}{\rho_0} \right)} \right]}{\partial x_j} - \epsilon$$
 (8)

where,

 ϵ is the SGS dissipation rate.

B. Non-Intrusive ROM-LSTM Methodology

As outlined in Algorithm 1, we initially obtain the time dependent modal coefficients by performing a POD transform on the snapshot data of the fluctuations. These are calculated from the Large Eddy Simulation data by subtracting the mean flow field values. An optimal number of these modal coefficients based on their relative information content are used for training a Recurrent Neural Network. Recurrent Neural Networks are a widely used neural network architecture in cases where the output information is dependent on current input as well as characteristics learnt from previous observations. RNNs contain cyclic or recurrent connections that enable them to continuously learn characteristics from a series of data and predict future outcomes. Closely following [27], we use Long Short-Term Memory (LSTM) neural networks, a special variant of RNN architecture better suited for learning long-term dependencies in the input data. After the network is trained we predict the modal coefficients for required number of snapshots. These are then used to project the modal coefficients using the POD basis back to fluctuation field snapshots. We can then calculate the data field using the previous average calculated.

Algorithm 1 ROM-LSTM approach

- 1: Obtain 3D solution data from Large Eddy Simulations for the domain of interest.
- 2: Compute the fluctuation flow field for the given number of snapshots, i.e. mean-subtracted flow field

$$\overline{u}(x, y, z, t_n) = \frac{1}{N} \sum_{n=1}^{N} u(x, y, z, t_n)$$

$$u'(x, y, z, t_n) = u(x, y, z, t_n) - \overline{u}(x, y, z, t_n)$$

3: Compute the POD basis for the data matrix A made up from the snapshots data using Singular Value Decomposition.

$$\mathbf{A} = \mathbf{\Phi} \mathbf{\Sigma} \mathbf{V}$$

Where Φ is the basis vectors matrix, Σ is a diagonal matrix with singular values.

- 4: Using relative information content of singular values, pick the optimal number of POD modes and basis vectors.
- 5: Find the modal coefficients using the optimal basis vectors matrix Φ_w and data matrix A,

$$\mathbf{C} = \mathbf{A}^T \mathbf{\Phi}_w$$

- 6: Pre-process the data by scaling and re-arranging data for LSTM training with appropriate look-back window.
- 7: Predict the modal coefficients with the trained network for future snapshots.
- 8: Using the optimal basis vectors calculate the fluctuation field, U'

$$\mathbf{U}' = \Phi_w \mathbf{C}^T$$

9: Compute the predicted flow field by adding the mean value to the predicted snapshot data.

IV. Results and Discussion

A. Simulation Setup

For this study we setup a cubic building of height H in a three-dimensional domain for Large Eddy Simulation. We closely follow the recommendations of Franke et al.[33], Murakami and Mochida[34] for setting up the computational domain and initial flow conditions. Vertical profile proportional to $z^{1/4}$ [34] till a height of 2H, similar to the setup of Tutar and Oguz [35] was used for x-component of velocity u, with other components v, w set as zeros. Isotropic mesh resolution of H/10 was used with the upstream wind velocity at height H as 8m/s. Further details about the domain is tabulated in table 1 and presented in Fig 1. Neutral and dry atmospheric conditions were chosen with Coriolis parameter of 7.3×10^{-5} with boundary conditions on the top and bottom (z-direction) as free-slip and no-slip, left and right (x-direction) as inflow and outflow, front and back (y-direction) as outflows respectively.

Domain size	Specification
upstream (x-direction)	2H
downstream (x-direction)	7H
lateral (y-direction)	2.5H
above building (z-direction)	5H

Table 1 Domain details

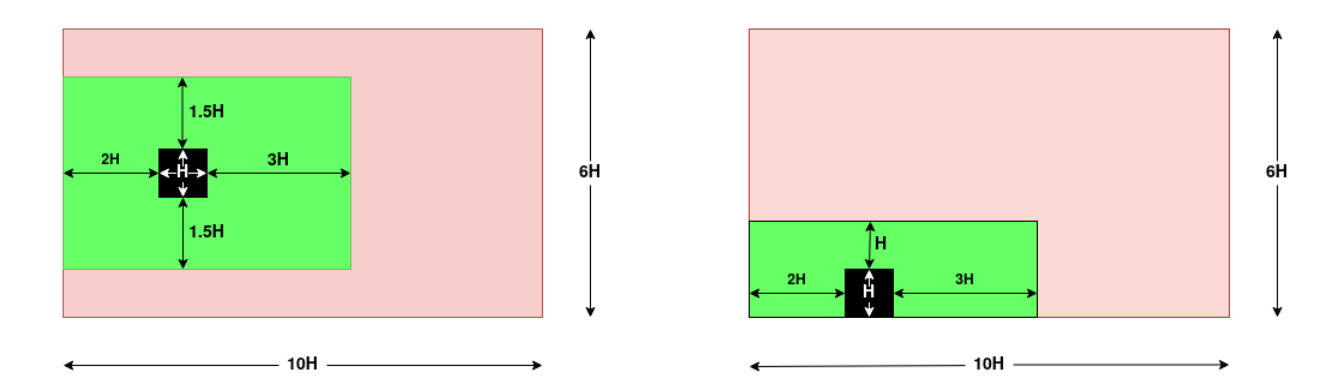


Fig. 1 Left-Top view (xy-plane); Right-Side view(xz-plane) of the domain; Green-domain of interest, Red-total domain for LES

B. ROM-LSTM results

Since the domain used for Large Eddy Simulation is relatively large we pick a smaller sub-domain of interest as depicted in Fig 1 for demonstrating the method. Furthermore the CFD simulation is run till 120 sec before the LES data is obtained for our study to let the simulation develop and reach a quasi-steady state inside the domain. Large Eddy Simulation data from this smaller domain is used as the input data for ROM-LSTM. To further simplify the model only the x-component of velocity u is utilized for this work. We obtain the three-dimensional simulation data from this smaller domain at every 1 second, hence forth this data will be referred to as snapshot data. Following Algorithm 1, we pick a threshold for relative information content as 80% giving us 28 modes as shown in Fig 2. We could notice from the comparison in fig. 3 for the first snapshot that, as expected although the finer details of the flow are lost, the major features still seem to be well represented. The LSTM neural network is trained on the snapshot data for 400 seconds and predictions are made for 100 more seconds, some more details about the neural network architecture is listed in table 2.

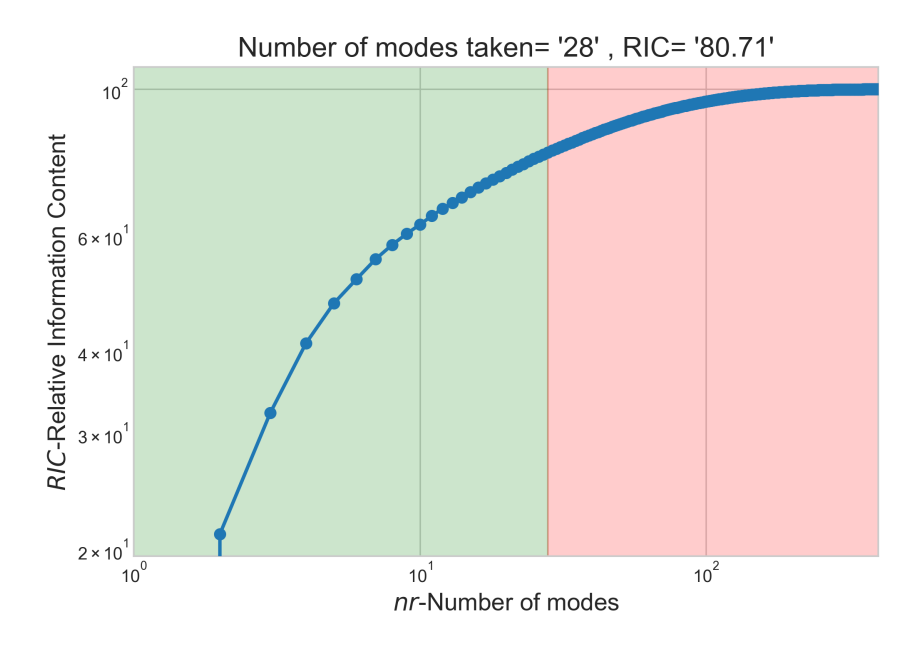


Fig. 2 Modes and their Relative Information Content; green-modes taken, red-modes neglected

Parameter	Specification
Number of hidden layers	2
Number of neurons in each hidden layer	64
Activation function	tanh
Lookback time-window	20
Recurrent dropout	0.2
Neuron dropout	0.2
Loss function	MSE
Optimiser	ADAM
Training-testing ratio	4:1

Table 2 Neural Network details

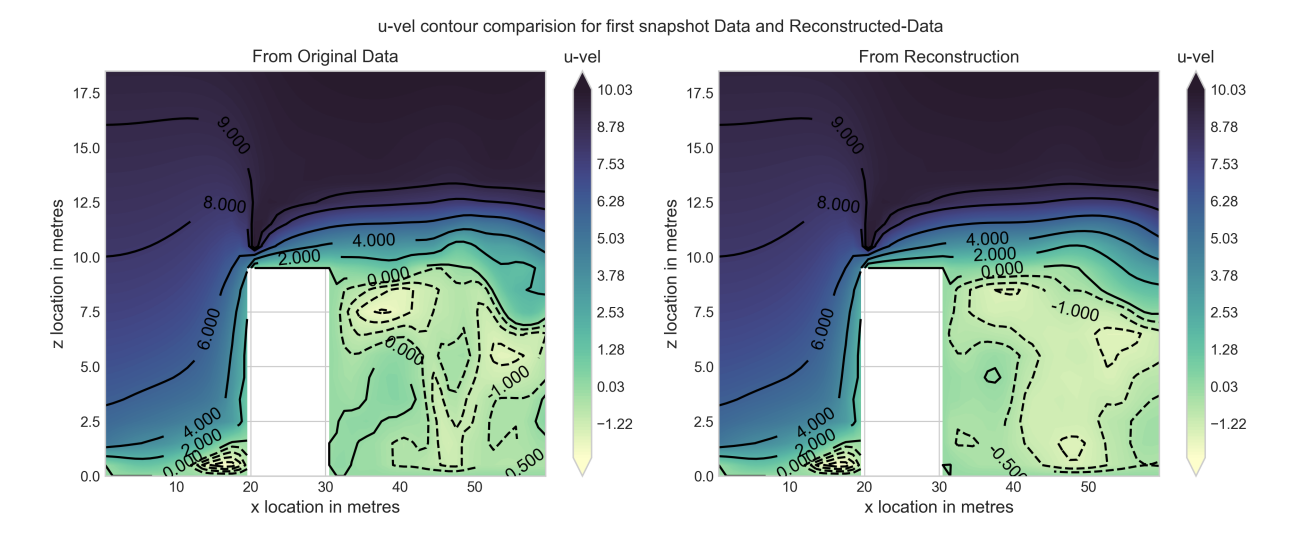


Fig. 3 u-velocity contour in XZ plane at the center of domain, for first snapshot

A comparison is made between the true modal coefficients and ROM-LSTM predictions in fig. 4 for the first 8 modes based on relative information content. We can see a close agreement in the modal coefficient predictions between the ROM-LSTM model and the true modes from the POD decomposition. Although there is slight mismatch in the amplitudes for all modes, the initial important modes seem to be in good agreement and it slowly deviates for the other modes. A contour plot in xz direction in the center of domain is also plotted for comparison between the predicted u-velocity field and the POD reconstructed field from LES data in fig. 5. It could be noticed that there seems to be a mismatch between the finer structures in the contour plot but we seem to have similar larger structures in the snapshots of 400, 450 and 500. As expected the predictions are better at 400th snapshot and deviate slowly as the number of the snapshot increases. However, we still see a close resemblance between the predictions and the POD reconstructed data.

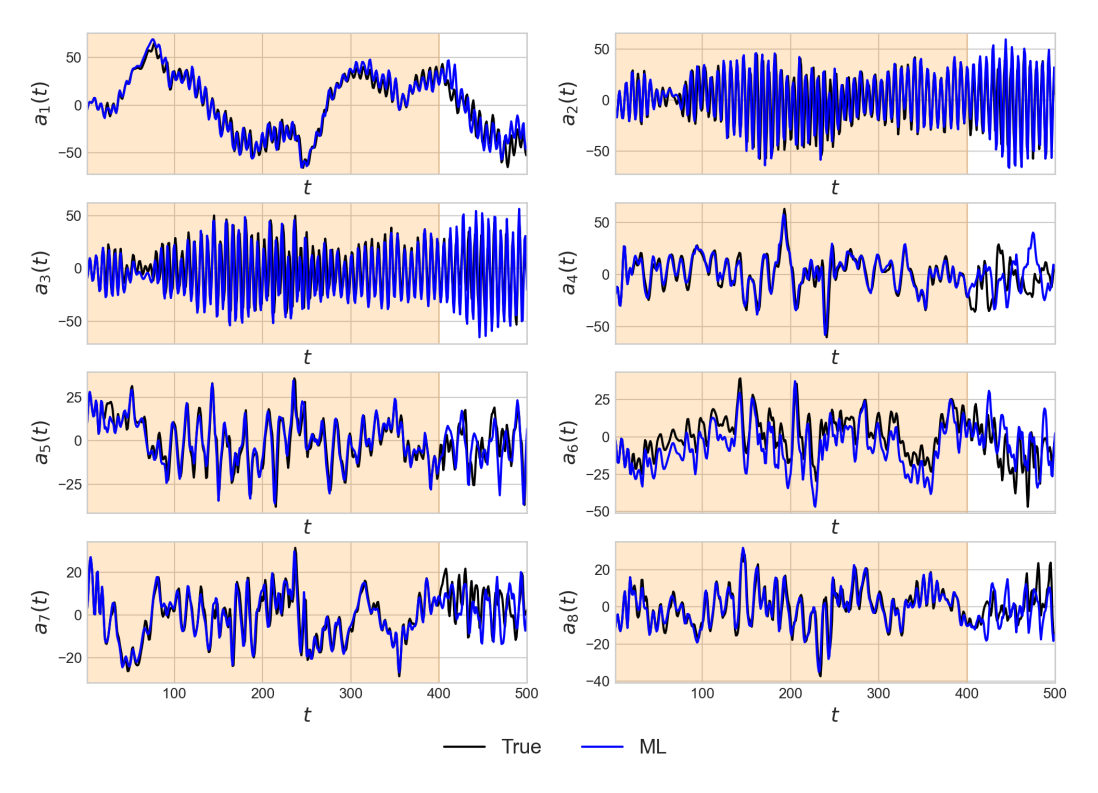


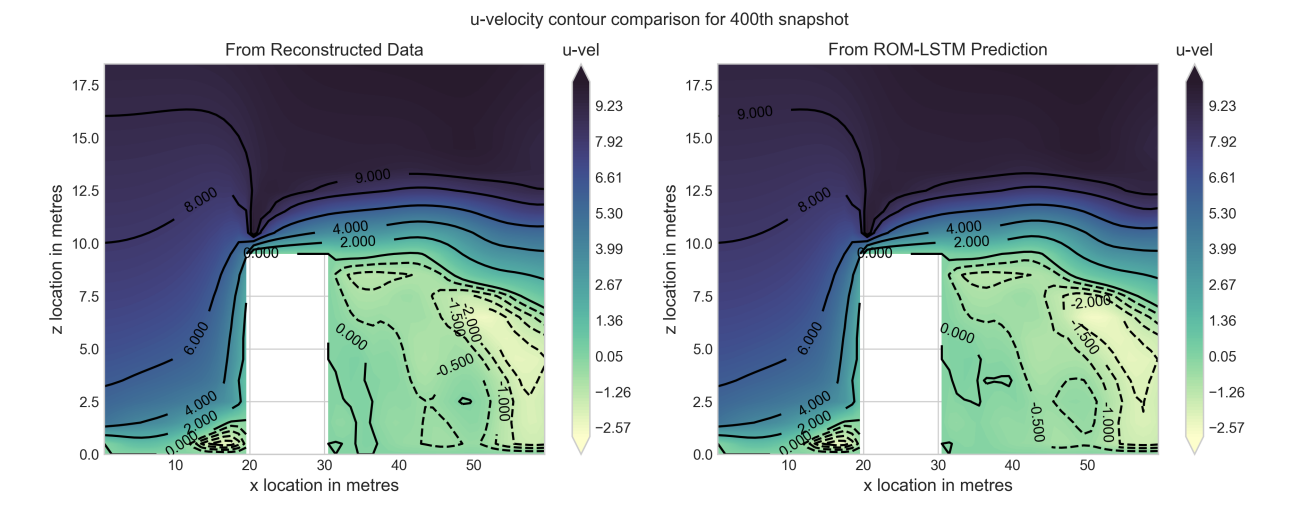
Fig. 4 Comparison between True and ROM-LSTM (ML) for first 8 modes for demonstration; Background colors: Tan/Orange - Training, White - Prediction

V. Conclusions and Future work

In this work we try to utilise an efficient, stable and robust fully non-intrusive ROM framework to aid us in realistic wind-data generation. We select a simplistic case of a cubic building in a wind flow and attempt to utilize this method as a demonstration for making some realistic predictions. This was pursued as a preliminary work before trying to extend the method to complex urban environment with multiple structures. Furthermore to simplify the model and setup, a smaller domain of interest was chosen and only the x-component of velocity, u was considered for predictions. We also simplify the atmospheric flow model for the LES simulations by choosing a neutral and dry atmospheric conditions eliminating the need to consider precipitation or different phases of water. This work could be extended further to make predictions for longer duration with data assimilation to reduce the error over-time. Furthermore, Convolutional Neural Networks could be used with Autoencoders to replace the Proper Orthogonal Decomposition based Reduced Order Model and also enable the Machine Learning model to understand the structures and terrain inside the domain, providing a unified framework for data-driven realistic wind field prediction for complex terrains in urban environments.

Acknowledgments

This material is based upon work supported by the National Science Foundation under Grant No. 1925147. Any opinions, findings, and conclusions or recommendations expressed in this material are those of the author(s) and do not necessarily reflect the views of the National Science Foundation. Some of the computing for this project was performed at the High-Performance Computing Center(HPCC) at Oklahoma State University supported in part through the National Science Foundation grant OAC-1531128. We would like to acknowledge high-performance computing support from Cheyenne[36] (doi:10.5065/D6RX99HX) provided by NCAR's Computational and Information Systems Laboratory, sponsored by the National Science Foundation.

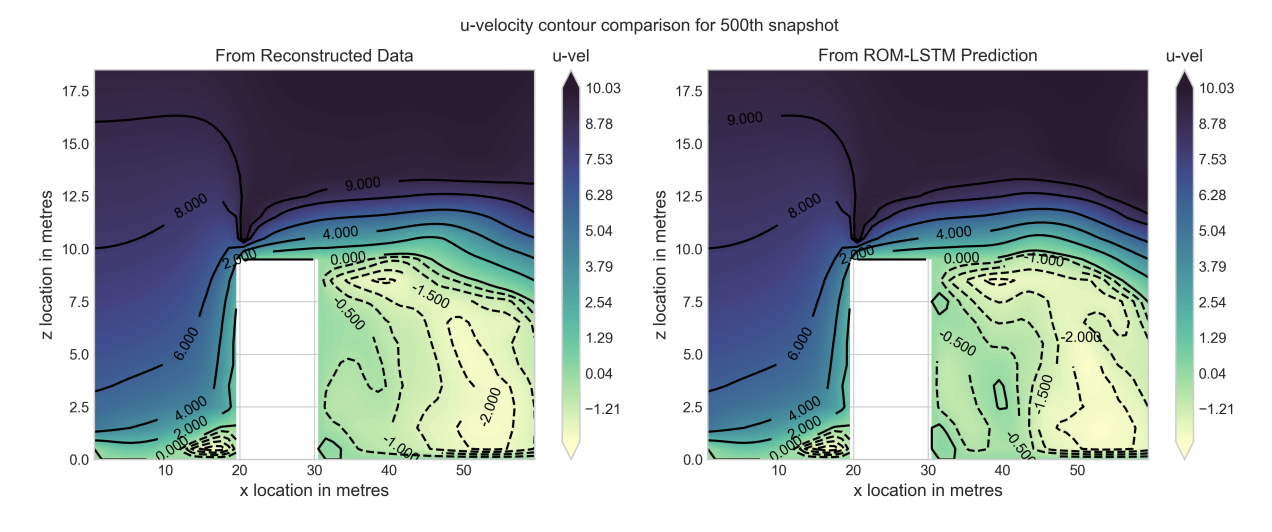


(a) u-velocity contour for xz plane in center of domain for 400th snapshot

u-velocity contour comparison for 450th snapshot From ROM-LSTM Prediction From Reconstructed Data u-vel 17.5 17.5 8.93 15.0 15.0 7.66 7.66 12.5 In a location in metres 2 z location in metres z location in metres z 12.5 6.39 6.39 5.12 5.12 3.85 3.85 2.59 2.59 1.32 1.32 5.0 5.0 0.05 0.05 -1.22 -1.22 -2.49 -2.49 30 10 x location in metres x location in metres

(b) u-velocity contour for xz plane in center of domain for $450 th \ snapshot$

1



(c) 500th snapshot

Fig. 5 u-velocity contour for xz plane in center of domain for 500th snapshot

References

- [1] Organization, I. C. A., Unmanned aircraft systems (UAS), International Civil Aviation Organization, Montreal, 2011.
- [2] Austin, R., Unmanned aircraft systems: UAVS design, development and deployment, Vol. 54, John Wiley & Sons, 2011.
- [3] Murphy, D. W., and Cycon, J., "Applications for mini VTOL UAV for law enforcement," *Sensors, C3I, information, and training technologies for law enforcement*, Vol. 3577, International Society for Optics and Photonics, 1999, pp. 35–43.
- [4] de Oliveira Silva, L., de Mello Bandeira, R. A., and Campos, V. B. G., "The use of UAV and geographic information systems for facility location in a post-disaster scenario," *Transportation Research Procedia*, Vol. 27, 2017, pp. 1137–1145.
- [5] Grubesic, T. H., and Nelson, J. R., "UAS Platforms and Applications for Mapping and Urban Analysis," *UAVs and Urban Spatial Analysis*, Springer, 2020, pp. 13–29.
- [6] León, C. D., "Drone Delivery? Amazon Moves Closer With F.A.A. Approval,", Aug 2020. URL https://www.nytimes.com/2020/08/31/business/amazon-drone-delivery.html.
- [7] Roth, M., "Review of atmospheric turbulence over cities," *Quarterly Journal of the Royal Meteorological Society*, Vol. 126, No. 564, 2000, pp. 941–990.
- [8] Arnfield, A. J., "Two decades of urban climate research: a review of turbulence, exchanges of energy and water, and the urban heat island," *International Journal of Climatology: a Journal of the Royal Meteorological Society*, Vol. 23, No. 1, 2003, pp. 1–26.
- [9] Onishi, A., Cao, X., Ito, T., Shi, F., and Imura, H., "Evaluating the potential for urban heat-island mitigation by greening parking lots," *Urban forestry & Urban greening*, Vol. 9, No. 4, 2010, pp. 323–332.
- [10] Corburn, J., "Cities, climate change and urban heat island mitigation: Localising global environmental science," *Urban studies*, Vol. 46, No. 2, 2009, pp. 413–427.
- [11] Agarwal, M., and Tandon, A., "Modeling of the urban heat island in the form of mesoscale wind and of its effect on air pollution dispersal," *Applied Mathematical Modelling*, Vol. 34, No. 9, 2010, pp. 2520–2530.
- [12] Kastner-Klein, P., Berkowicz, R., and Britter, R., "The influence of street architecture on flow and dispersion in street canyons," *Meteorology and Atmospheric Physics*, Vol. 87, No. 1-3, 2004, pp. 121–131.
- [13] Siqueira, J. C. D. C., "Modeling of wind phenomena and analysis of their effects on UAV trajectory tracking performance," Statler College of Engineering and Mineral Resources, 2017.
- [14] Raza, S. A., "Autonomous UAV control for low-altitude flight in an urban gust environment," Ph.D. thesis, Carleton University, 2015.
- [15] Salim, S. M., Buccolieri, R., Chan, A., and Di Sabatino, S., "Numerical simulation of atmospheric pollutant dispersion in an urban street canyon: Comparison between RANS and LES," *Journal of Wind Engineering and Industrial Aerodynamics*, Vol. 99, No. 2-3, 2011, pp. 103–113.
- [16] Tabassum, A., Vuppala, R. K., Bai, H., and Kara, K., "Variance Reduction of Quadcopter Trajectory Tracking under Stochastic Wind Disturbances," *arXiv* preprint arXiv:2104.10266, 2021.
- [17] Vuppala, R. K. S. S., and Kara, K., "Large-Eddy Simulation of Atmospheric Boundary-Layer Gusts for Small Unmanned Air Systems," *Bulletin of the American Physical Society*, 2020.
- [18] Sutherland, M., "Urban wake field generation using LES for application to quadrotor flight," Ph.D. thesis, Carleton University, 2015.
- [19] Lang, Y.-d., Malacina, A., Biegler, L. T., Munteanu, S., Madsen, J. I., and Zitney, S. E., "Reduced order model based on principal component analysis for process simulation and optimization," *Energy & Fuels*, Vol. 23, No. 3, 2009, pp. 1695–1706.
- [20] Noack, B. R., Morzynski, M., and Tadmor, G., Reduced-order modelling for flow control, Vol. 528, Springer Science & Business Media, 2011.
- [21] Xie, X., Mohebujjaman, M., Rebholz, L. G., and Iliescu, T., "Data-driven filtered reduced order modeling of fluid flows," *SIAM Journal on Scientific Computing*, Vol. 40, No. 3, 2018, pp. B834–B857.

- [22] Davoudi, B., Taheri, E., Duraisamy, K., Jayaraman, B., and Kolmanovsky, I., "Quad-rotor flight simulation in realistic atmospheric conditions," AIAA Journal, Vol. 58, No. 5, 2020, pp. 1992–2004.
- [23] Tracey, B. D., Duraisamy, K., and Alonso, J. J., "A machine learning strategy to assist turbulence model development," *53rd AIAA aerospace sciences meeting*, 2015, p. 1287.
- [24] Zhu, L., Zhang, W., Kou, J., and Liu, Y., "Machine learning methods for turbulence modeling in subsonic flows around airfoils," *Physics of Fluids*, Vol. 31, No. 1, 2019, p. 015105.
- [25] Maulik, R., Sharma, H., Patel, S., Lusch, B., and Jennings, E., "Accelerating RANS turbulence modeling using potential flow and machine learning," arXiv preprint arXiv:1910.10878, 2019.
- [26] Thuerey, N., Weißenow, K., Prantl, L., and Hu, X., "Deep learning methods for Reynolds-averaged Navier-Stokes simulations of airfoil flows," AIAA Journal, Vol. 58, No. 1, 2020, pp. 25–36.
- [27] Rahman, S. M., Pawar, S., San, O., Rasheed, A., and Iliescu, T., "Nonintrusive reduced order modeling framework for quasigeostrophic turbulence," *Physical Review E*, Vol. 100, No. 5, 2019, p. 053306.
- [28] Maronga, B., Gryschka, M., Heinze, R., Hoffmann, F., Kanani-Sühring, F., Keck, M., Ketelsen, K., Letzel, M. O., Sühring, M., and Raasch, S., "The Parallelized Large-Eddy Simulation Model (PALM) version 4.0 for atmospheric and oceanic flows: model formulation, recent developments, and future perspectives," *Geoscientific Model Development*, Vol. 8, No. 8, 2015, pp. 2515–2551.
- [29] Schumann, U., "Subgrid scale model for finite difference simulations of turbulent flows in plane channels and annuli," *Journal of Computational Physics*, Vol. 18, No. 4, 1975, pp. 376–404. https://doi.org/https://doi.org/10.1016/0021-9991(75)90093-5, URL https://www.sciencedirect.com/science/article/pii/0021999175900935.
- [30] Deardorff, J. W., "Stratocumulus-capped mixed layers derived from a three-dimensional model," *Boundary-Layer Meteorology*, Vol. 18, No. 4, 1980, pp. 495–527.
- [31] Wyngaard, J., Peltier, L., and Khanna, S., "LES in the surface layer: Surface fluxes, scaling, and SGS modeling," *Journal of the atmospheric sciences*, Vol. 55, No. 10, 1998, pp. 1733–1754.
- [32] Saiki, E. M., Moeng, C.-H., and Sullivan, P. P., "Large-eddy simulation of the stably stratified planetary boundary layer," *Boundary-Layer Meteorology*, Vol. 95, No. 1, 2000, pp. 1–30.
- [33] Franke, J., Hellsten, A., Schlünzen, K., and Carissimo, B., "Best practice guideline for the CFD simulation of flows in the urban environment-a summary," 11th Conference on Harmonisation within Atmospheric Dispersion Modelling for Regulatory Purposes, Cambridge, UK, July 2007, Cambridge Environmental Research Consultants, 2007.
- [34] Murakami, S., and Mochida, A., "3-D numerical simulation of airflow around a cubic model by means of the k-e model," *Journal of Wind Engineering and Industrial Aerodynamics*, Vol. 31, No. 2-3, 1988, pp. 283–303.
- [35] Tutar, M., and Oguz, G., "Large eddy simulation of wind flow around parallel buildings with varying configurations," Fluid Dynamics Research, Vol. 31, No. 5-6, 2002, p. 289.
- [36] Computational, and Laboratory, I. S., "Cheyenne: HPE/SGI ICE XA System (University Community Computing),", 2017.